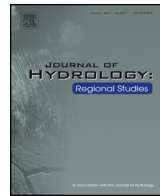




Contents lists available at ScienceDirect

Journal of Hydrology: Regional Studies

journal homepage: www.elsevier.com/locate/ejrh



Sources and spatial variability of groundwater-delivered nutrients in Maunalua Bay, O'ahu, Hawai'i



Christina M. Richardson ^{a,*}, Henrietta Dulai ^a, Robert B. Whittier ^b

^a Department of Geology and Geophysics, University of Hawai'i at Mānoa, 1680 East-West Road, Honolulu, HI 96822, United States

^b Department of Health, Safe Drinking Water Branch, State of Hawai'i, 919 Ala Moana Boulevard, Honolulu, HI 96814, United States

ARTICLE INFO

Article history:

Received 3 July 2015

Received in revised form 24 October 2015

Accepted 10 November 2015

Available online 12 December 2015

Keywords:

Submarine groundwater discharge

Wastewater

Nitrate stable isotope ratios

Nutrients

Island hydrogeology

On-site disposal systems

ABSTRACT

Study region: Maunalua Bay, O'ahu, Hawai'i.

Study focus: We examined submarine groundwater discharge (SGD), terrestrial groundwater, and nearshore marine water quality in two adjacent aquifers (Waialae East and Waialae West) with differing land-use and hydrogeologic characteristics to better understand the sources and spatial variability of SGD-conveyed nutrients. Nutrient concentrations and NO_3^- stable isotope ratios were measured and integrated with SGD flux, land-use, and recharge data to examine SGD nutrient loads and potential sources in each aquifer.

New hydrological insights for the region: Regionally elevated NO_3^- concentrations (166–171 μM) and $\delta^{15}\text{N}-\text{NO}_3^-$ values (10.4–10.9‰) were apparent in SGD in the Waialae West Aquifer, an area with high on-site disposal system density (e.g., cesspools). Coastal sites sampled in the neighboring Waialae East Aquifer exhibited significantly lower values for these parameters, with $\delta^{15}\text{N}-\text{NO}_3^-$ values ranging from 5.7–5.9‰ and NO_3^- concentrations from 43–69 μM . The isotopic composition of NO_3^- in SGD originating from the Waialae West Aquifer was consistent with wastewater. Modeled recharge data corroborated the NO_3^- stable isotope source designation. SGD emanating from Waialae West Aquifer was primarily influenced by two-component mixing of a wastewater source with low nutrient groundwater as wastewater effluent accounted for more than 4% of total recharge and 54–95% of total N and P loads in the aquifer.

© 2015 The Authors. Published by Elsevier B.V. This is an open access article under the CC BY-NC-ND license (<http://creativecommons.org/licenses/by-nc-nd/4.0/>).

1. Introduction

Global declines in coral reef abundance are closely associated with increasing human pressures (Hughes et al., 2003; Pandolfi et al., 2003). Projected trends of ocean warming and acidification will exacerbate coral reef degradation, creating adverse human and ecological consequences in locations such as the Hawaiian Islands where economic benefits of coral reefs are estimated to exceed \$360 million yr⁻¹ (Cesar and Van Beukering, 2004; Nicholls et al., 2007). Corals face additional local stressors which may intensify climate change induced effects and act synergistically to alter benthic community structure

Abbreviations: ANOVA, analysis of variance; CTD, conductivity-temperature-depth; DIN, dissolved inorganic nitrogen; HSD, honestly significant difference; OSDS, on-site disposal system; SGD, submarine groundwater discharge; SD, standard deviation; TDN, total dissolved nitrogen; TDP, total dissolved phosphorous.

* Corresponding author.

E-mail address: cmrich@hawaii.edu (C.M. Richardson).

(Ateweberhan et al., 2013; Smith et al., 2001). The impact of local stressors such as water pollution on coral health will rise as anthropogenic disturbances persist in the coastal environment.

Nutrient pollution of coastal waters may arise from terrestrial non-point sources of N and P such as OSDS and fertilizer leachate. SGD is widely recognized as an important conduit for the transport of land-sourced N and P to coastal environments (Beusen et al., 2013; Moore, 1999; Paytan et al., 2006; Rodellas et al., 2015; Slomp and Van Cappellen, 2004). SGD water and nutrient inputs are comparable to surface water contributions in many coastal areas (Corbett et al., 1999; Hwang et al., 2005; Johannes, 1980; Krest et al., 2000; Lapointe and Clark, 1992; Taniguchi et al., 2008). Sustained nutrient loading of marine waters through SGD may promote critical ecological phase shifts in nearshore reef flats, both directly and indirectly, shifting dominance from coral to algae in systems with low grazing pressures (McCook, 1999). Deciphering the magnitude of SGD and associated interactions between SGD-derived nutrients and biological productivity is challenging, however, and the role of groundwater as a land-ocean pathway for nutrients into coral reefs remains poorly understood.

Groundwater fluxes to the coastal waters of Hawai'i can be substantial in the context of global SGD rates (Ganguli et al., 2014; Kim et al., 2003; Knee et al., 2010; Lee and Kim, 2007; Swarzenski et al., 2013). Moreover, much of this SGD is derived from shallow, unconfined basal aquifers that are especially susceptible to anthropogenic effects. OSDS leachate, which consists of household waste leaking to the water table from underground pits, represents a potential vector of anthropogenic N and P to Hawai'i's basal aquifers and their attendant SGD. O'ahu's dramatic population growth in the past century has resulted in concentrated areas of OSDS island-wide (Whittier and El-Kadi, 2009). The effects of high OSDS density on proximal coastal water quality are unknown.

Elevated nutrient loading of SGD has been documented near the western edge of Maunalua Bay, O'ahu, an area with high OSDS density. Historically, Maunalua Bay was a vital economic and recreational resource in the Hawaiian Islands, supporting fishpond aquaculture during the 18–20th centuries (Atkinson, 2007). Widespread declines in coral reef coverage have been linked to urbanization of Maunalua Bay and, indirectly, overfishing (Wolanski et al., 2009). Ongoing reef degradation is primarily attributed to sediment runoff and nutrient loading of streams and groundwater discharging into the bay (Dimova et al., 2012; Ganguli et al., 2014; Swarzenski et al., 2013; Wolanski et al., 2009). The sources of these nutrients and the spatial variability of SGD nutrient fluxes across the bay remain unclear.

In this study, we address issues in determining nutrient sources and variability within the bay by using stable isotope ratios of ^{15}N and ^{18}O of NO_3^- as a proxy for NO_3^- source. Analysis of $\delta^{15}\text{N}-\text{NO}_3^-$ and $\delta^{18}\text{O}-\text{NO}_3^-$ values can provide diagnostic data for inferring N sources and stages of N cycling in aquatic environments (Kendall and McDonnell, 1998). NO_3^- concentrations coupled with NO_3^- stable isotope data may yield evidence of anthropogenic perturbations in a range of physical settings (Aravena et al., 1993; Aravena and Robertson, 1998; Cole et al., 2006; McClelland et al., 1997). This study aims to examine the relationship between land-use and SGD composition in Maunalua Bay by: (1) sampling nutrient concentrations of groundwater and coastal waters to establish a baseline understanding of nutrient profiles across a salinity gradient, (2) monitoring SGD fluxes via ^{222}Rn in water time-series measurements to assess the spatial variability of nutrient delivery to these waters, and (3) utilizing $\delta^{15}\text{N}-\text{NO}_3^-$ and $\delta^{18}\text{O}-\text{NO}_3^-$ values in conjunction with land-use and recharge patterns to evaluate potential sources of N and P at each site.

2. Background

2.1. Study area

The study area was focused on regions of known SGD along the coastline of Maunalua Bay on the southeastern shore of O'ahu, Hawai'i (Fig. 1a). A preliminary salinity and ^{222}Rn survey of the Maunalua Bay coastline indicated that SGD is concentrated at three main locations: Black Point, Wailupe, and Kawaikui (Fig. 1b). These site locations exhibited low salinity and elevated ^{222}Rn activities during the survey, characteristics analogous to regions of SGD. Surface water inputs were negligible at all river mouths and drainages during the survey except for Wailupe Stream. Three upland wells (Aina Koa I, Aina Koa II, and Palolo Tunnel) were sampled to provide supplemental geochemical data for comparison to the coastal site groundwater endmembers (Fig. 1c). The Palolo Tunnel well, a horizontal shaft tapping high-level dike impounded groundwater, sits in the ridgeline of the Ko'olau Mountains and is located adjacent to the Waialae West Aquifer boundary. As the geochemical composition of high-level groundwater near the undeveloped Ko'olau crest is likely to be fairly uniform, we consider the Palolo Tunnel well to have a background terrestrial groundwater signature. The Aina Koa wells are located in the Waialae West Aquifer.

2.2. Geology

Maunalua Bay is an 8 km embayment flanked by remnants of rejuvenated stage volcanism at the base of the Ko'olau Mountains. Cinder cone vent deposits and tuff deposits enclose the perimeter of the bay (Stearns and Vaksvik, 1935). The Ka'au Rift Zone and a series of northeast trending dikes confine groundwater into two distinct areas in southeast O'ahu: Waialae East Aquifer and Waialae West Aquifer (Eyre et al., 1986; Takasaki and Mink, 1982). The Ka'au Rift further delineates the hydrogeologic boundaries of the southeastern section of the island by acting as a barrier to lateral groundwater flow between the groundwater division of Black Point and the surrounding watersheds west of Black Point. As such, Black Point's SGD is supplied by Waialae West Aquifer, an entirely separate aquifer than that of Wailupe and Kawaikui which reside in

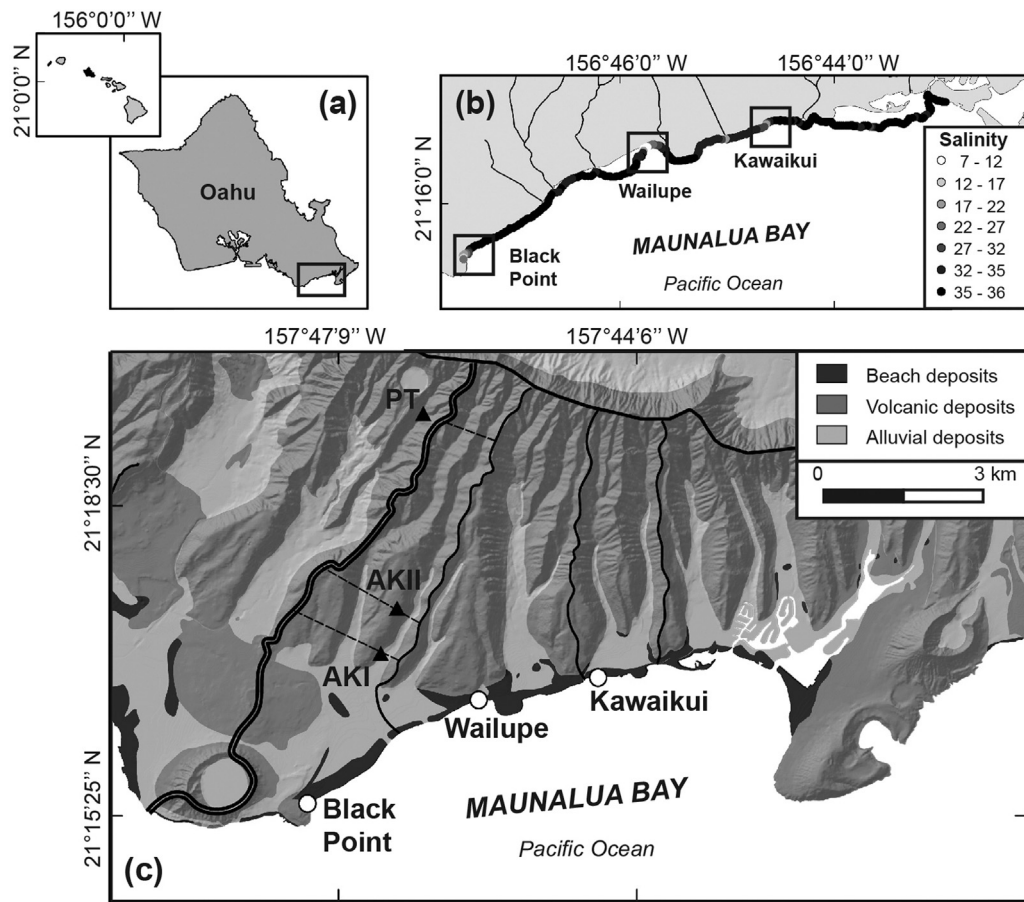


Fig. 1. (a) Overview of the Hawaiian Islands and O'ahu. Maunalua Bay is enclosed within the black box. (b) Coastline salinity survey of Maunalua Bay. (c) Simplified geologic map of Maunalua Bay, O'ahu. Coastal sites and well locations are shown as circular and triangular markers, respectively. Wells are symbolized as follows for all subsequent figures: AK I is Aina Koa I, AK II is Aina Koa II, and PT is Palolo Tunnel. Aquifer and watershed boundaries are represented by solid lines. The Ka'au Rift Zone is shown as a double solid line. Spatial boundaries used for recharge calculations are indicated by the dotted lines in the Waialae West Aquifer. The Waialae East Aquifer is separated into two subsections based on watershed boundaries which individually contain Wailupe and Kawaikui.

Waialae East Aquifer. Low- permeability alluvial deposits fill the valley regions of the Ko'olau Mountains in the study area ([Eyre et al., 1986](#)). Regions of SGD in Maunalua Bay tend to fall in places where volcanic, high-permeability rocks outcrop near the coast as these deposits convey water readily compared to their alluvial counterparts ([Eyre et al., 1986](#)).

2.3. Hydrology

Runoff and recharge account for about 33% and 66% of total inflow (rain, fog, irrigation, septic, and direct recharge inputs) to the soil moisture zone reservoir excluding evapotranspiration in both aquifers, respectively ([Engott et al., 2015](#)). As such, SGD likely serves as the primary delivery mechanism of terrestrial water to the coast in this area. Groundwater is recharged primarily at high elevations in the Ko'olau Mountains and subsequently percolates through dike compartments into the freshwater basal lens of the island. Perennial water flow occurs exclusively at the headwaters of streams that intersect dike-impounded groundwater near the crest of the Ko'olau Mountains ([Eyre et al., 1986](#)). Streams are flashy and intermittent below their headwaters, discharging to the ocean only during periods of extended rainfall ([Takasaki and Mink, 1982](#)).

2.4. Climate

O'ahu experiences mild temperatures and moderate humidity year-round. Prevailing northeasterly winds are strongest during the summer (21 km hr^{-1}) and less substantial during winter (14 km hr^{-1}) ([Nichols et al., 1997](#)). Due to orographic effects, the southeastern region of O'ahu receives extremely variable amounts of precipitation. In the Black Point area, nearly 297 cm of rain fall annually at the crest of the Ko'olau Mountains, decreasing to 63 cm at the coast ([Giambelluca et al., 2013](#)). Likewise, the ridges of the Kawaikui and Wailupe area receive 195 cm of precipitation annually which drops to 80 cm at the

coast ([Giambelluca et al., 2013](#)). Precipitation is predominantly seasonal, with nearly 70% occurring during the months of October–April ([Nichols et al., 1997](#)).

3. Methods

3.1. Water sample collection and processing

Water samples were collected from coastal waters, submerged springs, beach piezometers, and upland wells during sampling events in January–April 2015. At each coastal site, grab samples were taken synchronously along five points of a shore perpendicular transect starting at the location of the groundwater seep or spring and extending out into marine waters. Transect lengths were selected to capture the full salinity gradient at each location. Transects extended offshore 120 m, 250 m, and 75 m for Black Point, Wailupe, and Kawaikui, respectively. Samples were taken at each transect point in time-series every hour over five–eight hours to capture the potential effects of tide, wind, and currents on observed nutrient profiles.

Samples were originally collected in acid-cleaned 500 mL HDPE bottles. Samples for nutrients, salinity, and NO_3^- stable isotope analyses were subsampled from the 500 mL bottles. Nutrient and NO_3^- stable isotope water samples were filtered through a 0.2 μm nylon filter into acid-cleaned 60 mL HDPE bottles. Nutrient samples were stored in a refrigerator at 4 °C and NO_3^- stable isotope samples were frozen at –20 °C immediately after collection. Three production wells were additionally sampled, with nutrient and NO_3^- stable isotope subsamples filtered at the point of collection using a 0.45 μm inline capsule filter. These well water samples were processed and stored as the coastal samples above.

Nutrient samples were analyzed for TDN, TDP, $\text{NO}_3^- + \text{NO}_2^-$, PO_4^{3-} , NH_4^+ , and SiO_4^{4-} using a SEAL AutoAnalyzer 3HR at the University of Hawai'i SOEST Laboratory for Analytical Biogeochemistry. $\text{NO}_3^- + \text{NO}_2^-$ concentrations were used as a direct proxy for NO_3^- concentration herein based on past data that indicate NO_2^- is consistently found in quantities below 0.2 μM at each site ([Holleman, 2011](#)). The procedures for TDN and TDP follow fully automated methods with on-line digestion as outlined in [Yu et al., 2004](#). NO_3^- , PO_4^{3-} , NH_4^+ , and SiO_4^{4-} were measured using the following established methods: [Armstrong et al., 1967](#); [Grasshoff et al., 2009](#); [Murphy and Riley, 1962](#); [Kéroutel and Aminot, 1997](#) and, [Grasshoff et al., 2009](#), respectively. Thirteen blind duplicates were partitioned from a total of 106 nutrient samples (Black Point, $n = 40$; Kawaikui, $n = 26$; and Wailupe, $n = 40$). Sample precision at one SD was as follows: 1.2 μM TDN, 0.06 μM TDP, 0.6 μM $\text{NO}_3^- + \text{NO}_2^-$, 0.01 μM PO_4^{3-} , 0.13 μM NH_4^+ , and 4 μM SiO_4^{4-} . Salinity samples were run on a Metrohm 856 Conductivity Module.

NO_3^- stable isotope samples were processed at the University of Hawai'i Stable Isotope Biogeochemistry Lab using denitrification methods ([Böhlke et al., 2003](#); [Casciotti et al., 2002](#); [McIlvin and Casciotti, 2010, 2011](#); [Sigman et al., 2001](#)). $\delta^{15}\text{N}-\text{NO}_3^-$ and $\delta^{18}\text{O}-\text{NO}_3^-$ values were measured using a Thermo Finnigan MAT 252 coupled with a GasBench II interface and presented in per mil notation (‰) with respect to AIR for $\delta^{15}\text{N}$ and VSMOW for $\delta^{18}\text{O}$ values. Nitrate stable isotope values were normalized to USGS-32/34/35 per [Böhlke et al. \(2003\)](#) and [McIlvin and Casciotti \(2011\)](#). Twelve duplicates were subsampled from a total of 57 NO_3^- stable isotope samples (Black Point, $n = 18$; Kawaikui, $n = 19$; Wailupe, $n = 14$; $n = 2$ for each well). Sample precision within one SD was 0.3‰ for $\delta^{15}\text{N}$ values and 0.4‰ for $\delta^{18}\text{O}$ values.

3.2. ^{222}Rn groundwater fluxes

SGD fluxes were calculated using in situ ^{222}Rn measurements during water sampling events at Black Point, Kawaikui, and Wailupe in January and April of 2015. An additional on-site monitoring station was set up at Black Point and Wailupe to establish a ^{222}Rn groundwater endmember using a piezometer installed in submerged springs at a depth of 1 m. Endmember ^{222}Rn time-series measurements were taken every thirty minutes for five hours at Black Point ($n = 10$) and seven hours at Wailupe ($n = 14$) during the water sampling period. ^{222}Rn grab samples were collected in 250 mL bottles over four hours from a beach spring at Kawaikui ($n = 3$) using a piezometer at 0.5 m depth and from each of the three wells ($n = 2$ for each well) for groundwater endmember determination. Grab samples were analyzed the same day using a radon in air monitoring system (RAD H₂O, Durridge) and decay-corrected. Groundwater endmember ^{222}Rn concentrations were averaged for each site for use in subsequent calculations.

A coastal surface water sampling station was positioned adjacent (within 15 m at Black Point, and 10 m at Kawaikui and Wailupe) to the groundwater source at each site. Water was continuously pumped from a fixed depth through an air–water exchanger and looped into a radon in air monitoring system (RAD AQUA, Durridge) for measurement at thirty minute integrated periods. ^{222}Rn in water activities were calculated by correcting ^{222}Rn in air measurements to salinity and temperature data recorded by a multi-parameter water quality probe ([Schubert et al., 2012](#)). A CTD diver was deployed during each time-series for depth-correction of ^{222}Rn inventories. Surface water ^{222}Rn inventories were used to calculate advection rates of groundwater at each site using a transient box model that accounts for ^{222}Rn evasion to the atmosphere, radioactive decay, and mixing losses ([Burnett et al., 2001](#); [Burnett and Dulaiova, 2003](#)).

3.3. Recharge model description

Total groundwater flux in the terrestrial domain of the study area was assumed to equal recharge as calculated by [Engott et al., 2015](#). Recharge was computed using a soil–water balance model with daily time-steps that capture the dynamic

Table 1

Mean and SD (1σ) of groundwater radon activities for each sampling location.

Site	Salinity	^{222}Rn activity dpm L^{-1}
Black Point ($n = 10$)	4.6	740 ± 11
Kawaikui ($n = 3$)	2.0	86 ± 18
Wailupe ($n = 14$)	2.3	250 ± 5
Palolo Tunnel ($n = 2$)	0.1	22 ± 12
Aina Koa I ($n = 2$)	0.4	150 ± 30
Aina Koa II ($n = 2$)	0.2	28 ± 9

relationship between rainfall, runoff, and evapotranspiration. Water inputs to the model include rainfall (Giambelluca et al., 2013), irrigation, and seepage rates from OSDS systems utilizing soil treatment (Whittier and El-Kadi, 2009). Water losses in the model include direct runoff and evapotranspiration (Giambelluca et al., 2014). The algebraic sum of the water inputs and water outputs were added to soil storage. Any amount that exceeded the soil storage capacity in the root zone was considered recharge. Seepage from cesspools to the aquifer was considered separately from direct recharge since the infiltration zone of these units is typically beneath the root zone where evapotranspiration will occur.

OSDS seepage rates were taken from Whittier and El-Kadi (2009). The number of OSDS units (cesspools, septic systems, aerobic, and soil units) were based on available wastewater records provided by the Hawai'i Department of Health supplemented by indirect methods that included analyzing building, property tax, and water billing records to identify parcels with wastewater disposal. The location of the candidate parcels was compared to sewer infrastructure coverages. Parcels within service areas were assumed to be connected to a sewer and removed from consideration. All parcels identified as having an OSDS using the indirect methods were further assumed to be served by cesspools, the dominant OSDS in Hawai'i. The effluent discharge rate for residential OSDS was assumed to be $0.75 \text{ m}^3 \text{ d}^{-1}$ based on current wastewater regulations (HDOH, 2004). For non-residential parcels, the effluent discharge rate was based on estimates in Metcalf and Eddy, 1991. The flux of N and P was incorporated into the recharge coverage by doing a spatial join of the OSDS coverage from Whittier and El-Kadi (2009). The join summed the N and P fluxes for all of the OSDS that fell within each recharge coverage polygon. This comprehensive recharge model was used herein to quantify the following for each aquifer or watershed: (1) the number and types of OSDS in each study area, (2) total recharge, (3) wastewater recharge, (4) background N and P loads, and (5) wastewater N and P loads.

3.4. Statistical analyses

One-way ANOVA was used to test for homogeneity in mean groundwater endmember compositions for inorganic nutrient concentrations and nitrate stable isotope values across site locations. A post hoc Tukey HSD analysis was performed when significant ($p < .01$) differences were detected. Tukey HSD results are reported at $p < .001$ as two asterisks (**) and $p < .05$ as one asterisk (*). Well geochemical data were not included in statistical analyses as sample size was limited.

4. Results

4.1. ^{222}Rn inventory and fluxes

SGD endmember ^{222}Rn in water activities ranged from 86 dpm L^{-1} at Kawaikui to 250 dpm L^{-1} at Wailupe, and 740 dpm L^{-1} at Black Point (Table 1). Terrestrial groundwater in the Black Point hydrogeologic subdivision, Waialae West Aquifer, revealed unique ^{222}Rn signatures that decrease with distance from the coast, from 150 dpm L^{-1} at Aina Koa I to

Table 2

SGD advection rates and corresponding shoreline fluxes to coastal waters. Mean advection rates include SD (1σ). Total flux is an estimate of site-wide SGD contributions.

Site	Advection rate			Shoreline flux $\text{m}^3 \text{ m}^{-1} \text{ d}^{-1}$	Shoreline length m	Total flux $\text{m}^3 \text{ d}^{-1}$
	Minimum m d^{-1}	Mean m d^{-1}	Maximum m d^{-1}			
Black Point	0.1	0.8 ± 0.4	2.3	51	300	15,000
Kawaikui	0.3	0.5 ± 0.3	0.6	25	200	5,000
Wailupe	0.4	1.1 ± 0.4	1.9	43	300	13,000

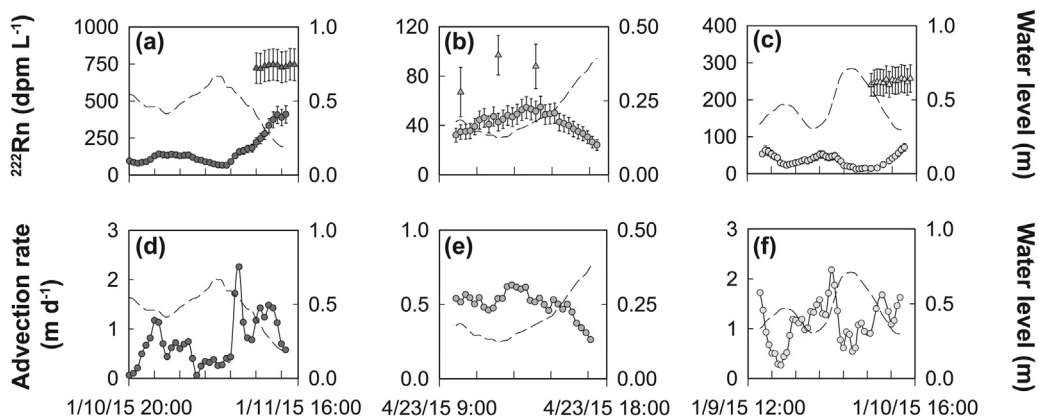


Fig. 2. Time-series ^{222}Rn in water values for (a) Black Point, (b) Wailupe, and (c) Kawaikui for the coastal sampling station (circular markers) and groundwater samples (triangular markers). Water level is represented by the dashed line. Error bars represent the SD (2σ) of ^{222}Rn measurements. Advection rates (circular markers) are plotted for (d) Black Point, (e) Wailupe, and (f) Kawaikui.

28 dpm L^{-1} at Aina Koa II. While ^{222}Rn activities peaked at Black Point, advection rates were highest at Wailupe on average (Table 2). Average advection rates ranged from 0.50 m d^{-1} at Kawaikui to 1.1 m d^{-1} at Wailupe. Black Point, Kawaikui, and Wailupe coastal surface water ^{222}Rn concentrations responded to changes in water level from tide while direct measurements of ^{222}Rn from the groundwater sources remained constant during the sampling periods, showing no tidal influence (Fig. 2). Advection rates were subsequently scaled to discharge rates using a conservative spatial estimate of the area of coastal waters that contributed to the measured ^{222}Rn activities. This estimate was determined using previous ^{222}Rn and salinity spatial surveys that depict areas of groundwater influence for Black Point, Wailupe (Nelson et al., 2015) and Kawaikui (Fig. 1b). Discharge rates were then divided by the width of the groundwater plume and scaled to shoreline fluxes. Shoreline fluxes were multiplied by the length of the shoreline thought to contribute SGD as estimated by the coastline salinity survey to calculate total SGD fluxes at each site. Total discharge rates varied site-to-site with Black Point conveying the largest volume of SGD to coastal waters at $15,000 \text{ m}^3 \text{ d}^{-1}$. Wailupe and Kawaikui SGD fluxes averaged $13,000 \text{ m}^3 \text{ d}^{-1}$ and $5000 \text{ m}^3 \text{ d}^{-1}$, respectively.

4.2. Nutrient concentrations in groundwater and coastal waters

As coastal groundwater endmembers varied in salinity spatially, measured water constituents were unmixed to a salinity of zero to establish analogous endmembers for comparison at all sites using the following equation:

$$C_1 = C_{\text{mix}} + (C_{\text{mix}} - C_2) \times \frac{(S_{\text{mix}} - S_1)}{(S_2 - S_{\text{mix}})} \quad (1)$$

where C_1 is the unmixed concentration, C_{mix} is the mixed concentration, C_2 is the marine endmember concentration, S_{mix} is the salinity of the mixed concentration, S_1 is the salinity of unmixed groundwater, and S_2 is the salinity of the marine endmember. Groundwater endmembers were calculated using the mean of five piezometer measurements at each site that were unmixed to a salinity of zero using Eq. (1) (Table 3). The marine endmembers were unique to each site and based on mean nutrient concentrations of the five most saline marine samples collected at each site.

Table 3

Mean groundwater (gw) and marine endmember nutrient composition at Black Point, Kawaikui, and Wailupe ($n=5$ for each site). Mean well nutrient compositions of Palolo Tunnel, Aina Koa I, and Aina Koa II are also included ($n=2$ for each well). Mean dissolved oxygen (DO) values are listed for all groundwater sampled.

Site	Salinity	TDN μM	TDP μM	PO_4^{3-} μM	SiO_4^{4-} μM	NO_3^- μM	NH_4^+ μM	DO Percent saturation
Black Point _{gw}	4.6	172	3.6	3.5	800	169	0.07	79.1
Black Point _{marine}	34.5	7	0.5	0.2	6	0.5	0.35	–
Kawaikui _{gw}	2.0	57	6.0	2.3	747	43	0.12	95.1
Kawaikui _{marine}	32.5	8	0.5	0.3	48	1.3	0.43	–
Wailupe _{gw}	2.3	72	2.0	1.9	781	69	0.08	93.4
Wailupe _{marine}	34.3	9	0.4	0.2	7	1.9	0.47	–
Palolo Tunnel	0.1	18	3.7	1.3	482	15	0.01	98.1
Aina Koa I	0.4	72	5.3	2.0	804	59	0.35	95.9
Aina Koa II	0.2	44	6.0	2.2	694	38	0.09	98.2

Table 4

Hypothetical freshwater endmembers at zero-salinity for Black Point, Kawaikui, and Wailupe. Tukey post hoc results are represented by two asterisks (**) for $p < .001$ and one asterisk (*) for $p < .05$. SD of mean endmember values are included for each constituent ($1\sigma, n = 5$).

Site	TDN μM	TDP μM	PO_4^{3-} μM	SiO_4^{4-} μM	NO_3^- μM	NH_4^+ μM
Black Point	$198 \pm 0.8^{**}$	$4.1 \pm 0.1^{**}$	$4.1 \pm 0.02^{**}$	$922 \pm 31^{**}$	$195 \pm 2.4^{**}$	0.03 ± 0.09
Kawaikui	$60 \pm 3.0^{**}$	$6.4 \pm 0.4^{**}$	$2.5 \pm 0.1^{**}$	$795 \pm 7^*$	$46 \pm 0.1^{**}$	0.14 ± 0.08
Wailupe	$76 \pm 1.3^{**}$	$2.1 \pm 0.1^{**}$	$2.1 \pm 0.03^{**}$	$835 \pm 14^*$	$74 \pm 2.4^{**}$	0.06 ± 0.07

Table 5

Nutrient fluxes at each site for TDN, TDP, PO_4^{3-} , SiO_4^{4-} , NO_3^- , and NH_4^+ using total SGD fluxes and groundwater endmember nutrient concentrations.

Site	TDN mol d ⁻¹	TDP mol d ⁻¹	PO_4^{3-} mol d ⁻¹	SiO_4^{4-} mol d ⁻¹	NO_3^- mol d ⁻¹	NH_4^+ mol d ⁻¹
Black Point	2,700	56	55	12,000	2,600	1.1
Kawaikui	290	30	12	3,800	220	0.6
Wailupe	970	27	26	11,000	930	1.1

Table 6

Average $\delta^{15}\text{N}-\text{NO}_3^-$ and $\delta^{18}\text{O}-\text{NO}_3^-$ values at each site. SD (1σ) of mean values are included for each location. Tukey post hoc results are displayed as two asterisks (**) for $p < .001$ and one asterisk (*) for $p < .05$. Wells were not included in statistical analyses as sample size was limited ($n = 2$).

Site	$\delta^{15}\text{N}$ ‰	$\delta^{18}\text{O}$ ‰
Black Point (n = 18)	$10.9 \pm 0.5^{**}$	$5.0 \pm 0.7^*$
Kawaikui (n = 19)	5.7 ± 0.4	3.4 ± 0.6
Wailupe (n = 14)	5.9 ± 0.7	3.5 ± 0.9
Aina Koa I (n = 2)	5.9 ± 0.1	4.7 ± 0.4
Aina Koa II (n = 2)	5.4 ± 0.1	3.2 ± 0.5
Palolo Tunnel (n = 2)	3.1 ± 0.1	2.0 ± 0.5

A one-way ANOVA showed significant spatial differences between groundwater endmembers ($F(2,12) = 12.97, p < .001$). Tukey HSD post hoc comparisons revealed that groundwater compositions differ significantly for all constituents except for NH_4^+ across sites ($p < .001, .05$). Black Point N species concentrations were nearly three times greater than Kawaikui and Wailupe, except for NH_4^+ which showed no spatial differences as concentrations were generally near detection limit. TDN levels ranged from 198 μM at Black Point to 60 μM and 76 μM at Kawaikui and Wailupe, respectively (Table 4). Nitrate content followed a similar trend to TDN at each site, ranging from 46–195 μM. Terrestrial well N species concentrations in Waialae West Aquifer were significantly lower than Black Point N species concentrations and fell more closely to Kawaikui and Wailupe endmember nutrient data for nearly all water constituents. Kawaikui and the terrestrial wells exhibited the highest TDP concentrations (3.7–6.4 μM) while PO_4^{3-} concentrations were highest at Black Point (4.1 μM).

Nutrient distributions were analyzed at each site relative to salinity and classified by examining their behavior with respect to a two-endmember mixing line that connects the groundwater and marine water endmembers at each site. Mixing lines were defined using the groundwater endmembers from Table 3. Deviations from this line in excess of two SD of the analytical and mixing line slope uncertainties were considered non-conservative. Mixing line slope uncertainty was included as groundwater and marine endmember variation may represent a source of error in residual values. NO_3^- concentrations were largely non-conservative at Black Point and Wailupe, and conservative at Kawaikui (Fig. 3). These non-conservative deviations were best exhibited by negative residuals in NO_3^- content in mid-salinity waters at Black Point and Wailupe. The positive residuals in NO_3^- content in mid-salinity waters at Kawaikui fell primarily within the thresholds set for conservative behavior. NH_4^+ concentrations deviated positively from mixing lines at all sites and were largely non-conservative at Black Point. TDP levels deviated from the predicted mixing lines at each site and PO_4^{3-} content showed non-conservative behavior across all sites (Fig. 4). SiO_4^{4-} content exhibited non-conservative behavior which peaked in brackish waters at Black Point and Wailupe. Kawaikui's distribution of SiO_4^{4-} concentrations appeared to be mostly conservative.

4.3. Coupling groundwater discharge to nutrient concentrations

SGD nutrient fluxes were calculated using the total SGD flux for each site and groundwater endmember nutrient concentrations from Table 3 (Table 5). SGD delivered nearly 2,700 mol d⁻¹ of TDN to the coast at Black Point while Wailupe averaged 970 mol d⁻¹. Kawaikui TDN fluxes were small in comparison, but still significant at 290 mol d⁻¹. NO_3^- fluxes

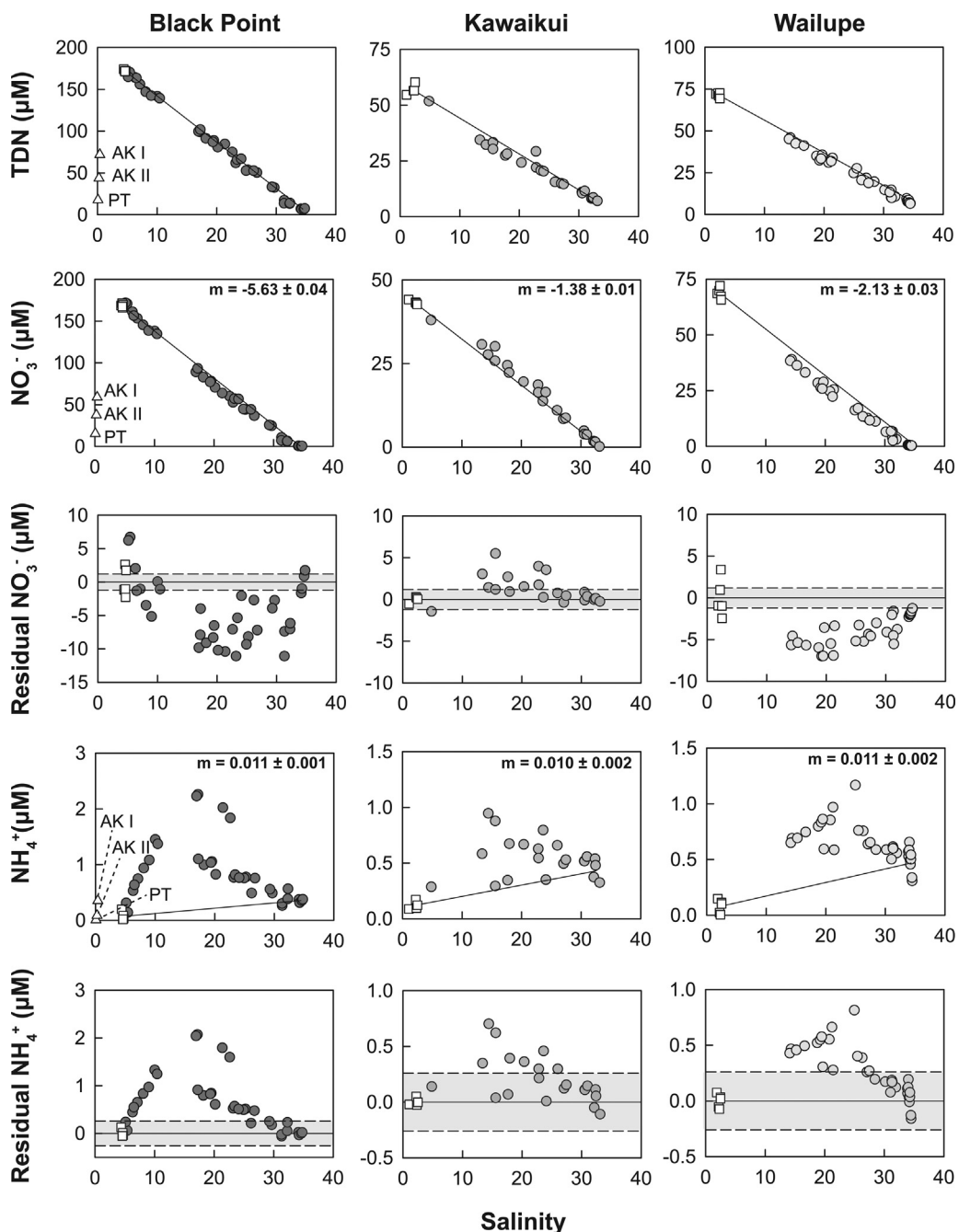


Fig. 3. TDN, NO₃⁻, residual NO₃⁻, NH₄⁺, and residual NH₄⁺ concentrations as a function of salinity by site. Solid lines represent conservative mixing lines between coastal groundwater and marine endmembers. Square and circular markers represent groundwater and coastal samples, respectively. Residuals refer to deviations from the mixing line. The slope (m) of the mixing lines used for residual calculations and the corresponding slope uncertainties are displayed in the upper right corner of relevant plots. Dashed lines represent the upper and lower boundaries of total uncertainty (2σ).

reflected observed trends in TDN fluxes. TDP and PO₄³⁻ fluxes were below 56 mol d⁻¹ at all sites. SiO₄⁴⁻ fluxes ranged from 3,800 to 12,000 mol d⁻¹ while NH₄⁺ fluxes were below 1.1 mol d⁻¹.

4.4. Spatial variability of NO₃⁻ stable isotopes

$\delta^{15}\text{N-NO}_3^-$ and $\delta^{18}\text{O-NO}_3^-$ values ranged from 3.1–11.8‰ and 2.0–6.7‰, respectively (Table 6). One-way ANOVA showed significant differences in NO₃⁻ stable isotope ratios between sites ($F(2,48)=8.01$, $p < .001$). Tukey HSD post hoc

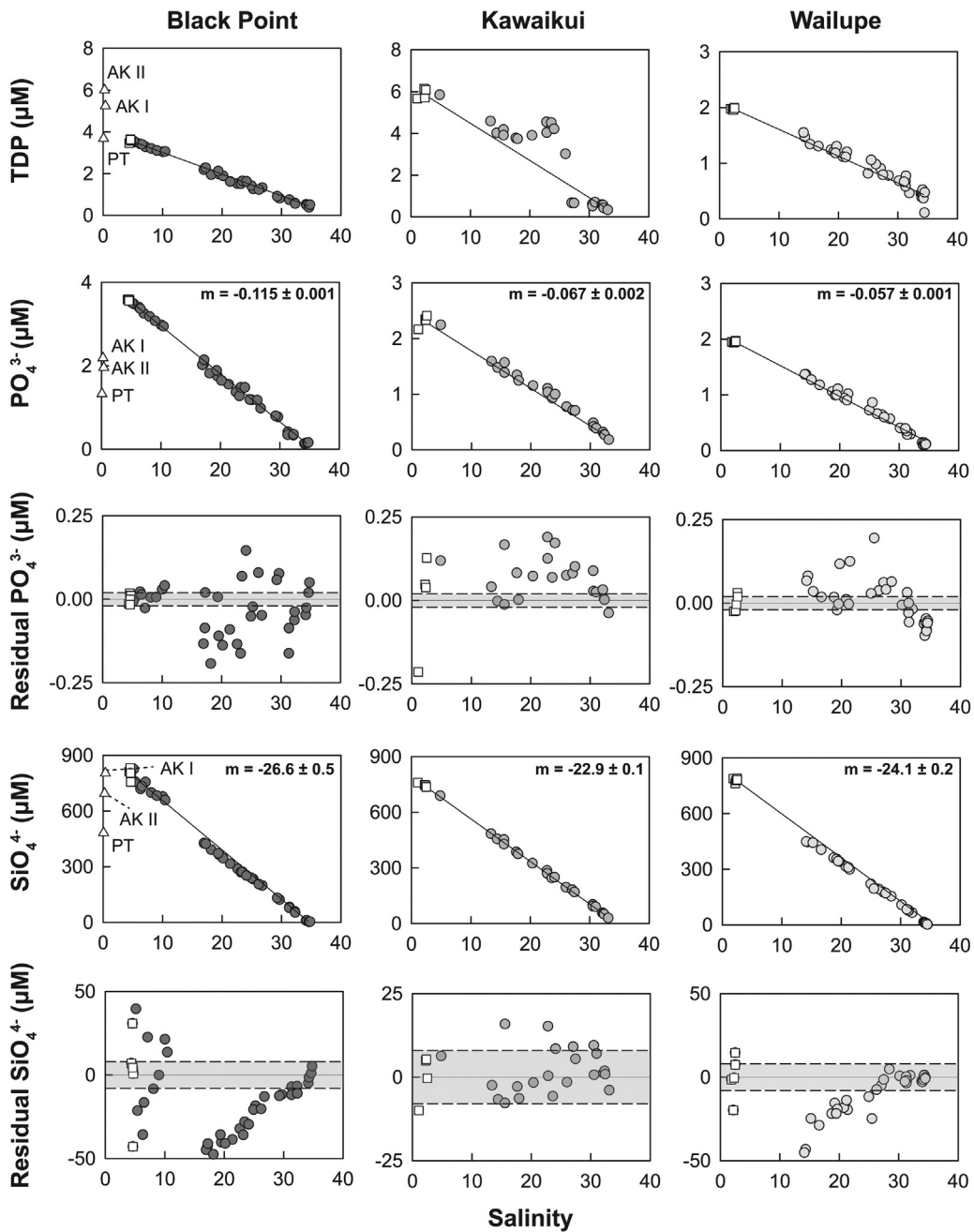


Fig. 4. TDP, PO_4^{3-} , residual PO_4^{3-} , SiO_4^{4-} and residual SiO_4^{4-} concentrations as a function of salinity by site. Solid lines represent conservative mixing lines between coastal groundwater and marine endmembers. Square and circular markers represent groundwater and coastal samples, respectively. Residuals refer to deviations from the mixing line. The slope (m) of the mixing lines used for residual calculations and the corresponding slope uncertainties are displayed in the upper right corner of the relevant plots. Dashed lines represent the upper and lower boundaries of total uncertainty (2σ).

results indicated that differences in Black Point spring and coastal water NO_3^- stable isotope values relative to Kawaikui and Wailupe were statistically significant ($p < .001$). Wailupe and Kawaikui overlapped in $\delta^{15}\text{N}-\text{NO}_3^-$ values while Black Point's values clustered independently (Fig. 5a). Black Point $\delta^{15}\text{N}-\text{NO}_3^-$ and $\delta^{18}\text{O}-\text{NO}_3^-$ values were invariable with NO_3^- concentration and elevated relative to Kawaikui and Wailupe (Fig. 5b). Similarly, Wailupe and Kawaikui NO_3^- stable isotope values were distributed uniformly across the NO_3^- gradient. The Aina Koa wells fell within the cluster of $\delta^{15}\text{N}-\text{NO}_3^-$ and $\delta^{18}\text{O}-\text{NO}_3^-$ values for Kawaikui and Wailupe. The Palolo Tunnel groundwater exhibited the lowest $\delta^{15}\text{N}-\text{NO}_3^-$ and $\delta^{18}\text{O}-\text{NO}_3^-$ values.

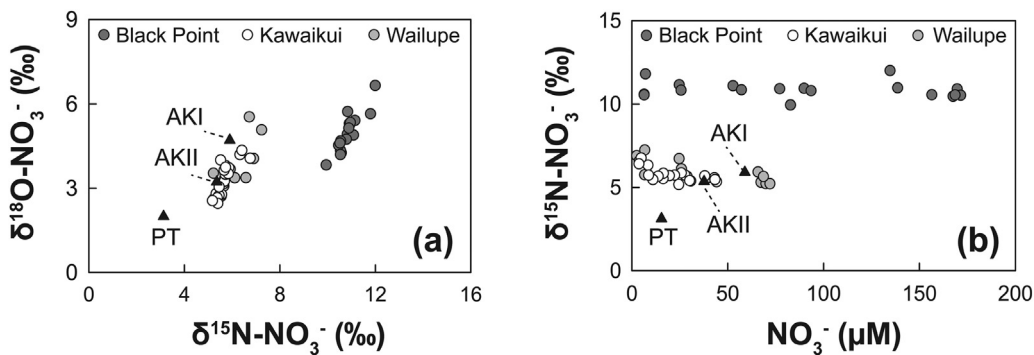


Fig. 5. (a) NO_3^- stable isotope ratios of ^{15}N and ^{18}O . (b) NO_3^- concentrations and $\delta^{15}\text{N-NO}_3$ values for all waters sampled.

5. Discussion

5.1. Magnitude of total SGD fluxes

SGD's influence on coastal waters in Maunalua Bay was largely site-dependent. While Black Point and Wailupe receive the majority of SGD via preferential flow conduits that manifest as discrete submarine springs, Kawaikui is a diffuse, seepage-dominated site with most groundwater percolating through layers of beach deposits before exiting to the ocean. Advection rates resembled those previously published for Maunalua Bay (Ganguli et al., 2014; Swarzenski et al., 2013). Total SGD fluxes were compared to recharge rates for each respective aquifer using the recharge model from Engott et al., 2015. For all subsequent calculations, Wailupe and Kawaikui recharge rates were defined by their respective watershed boundaries as the Waialae East Aquifer extends well east of the coastal sites sampled (Fig. 1c). In agreement with coastline survey ^{222}Rn and salinity data, the three sites sampled accounted for substantial portions (55–81%) of recharge in their hydrologic basins (Table 7). These values may be overestimated as modeled recharge rates do not include re-circulated seawater fluxes whereas total SGD fluxes incorporate both fresh and marine components.

5.2. Spatial distributions of geochemical parameters

Sites showed spatially distinct biogeochemical differences in coastal groundwater composition. SGD nutrient loadings were highest at Black Point for all water constituents. Nitrogen concentrations among the three coastal sites were locally-specific with Wailupe and Kawaikui most similar in N composition and indistinguishable in their $\delta^{15}\text{N-NO}_3$ (5.7–5.9‰) and $\delta^{18}\text{O-NO}_3$ (3.4–3.5‰) values. Similar to NO_3^- concentrations, $\delta^{15}\text{N-NO}_3$ ($10.9 \pm 0.5\text{‰}$) and $\delta^{18}\text{O-NO}_3$ ($5.0 \pm 0.7\text{‰}$) values were highest at Black Point, suggesting different terrestrial N sources or pathways from the other sites. Coastal groundwater ^{222}Rn activities were elevated at Black Point (740 dpm L^{-1}) relative to Kawaikui and Wailupe as well (86 – 250 dpm L^{-1}). The spatially-distinct geochemical signature of Black Point SGD may provide further insight into groundwater transit in the Waialae West Aquifer. Among the terrestrial wells, NO_3^- levels, ^{222}Rn activities, and NO_3^- stable isotope ratios increased with proximity to the coast. NO_3^- concentration and $\delta^{15}\text{N-NO}_3$ values increased from Palolo Tunnel ($15 \mu\text{M}$, $3.1 \pm 0.1\text{‰}$), an assumed terrestrial groundwater endmember for high-level, dike-confined water, to Aina Koa II ($38 \mu\text{M}$, $5.4 \pm 0.1\text{‰}$), the intermediate well in the flow path, and Aina Koa I ($59 \mu\text{M}$, $5.9 \pm 0.1\text{‰}$), the furthest down-gradient well sampled in the Waialae West Aquifer. Similarly, $\delta^{18}\text{O-NO}_3$ values revealed a progression from $2.0 \pm 0.5\text{‰}$ at Palolo Tunnel to $3.2 \pm 0.5\text{‰}$ at Aina Koa II and $4.7 \pm 0.4\text{‰}$ at Aina Koa I. Black Point's sustained high NO_3^- and PO_4^{3-} loading via SGD and the increase in $\delta^{15}\text{N-NO}_3$ values relative to the up-gradient terrestrial wells in the Waialae West Aquifer indicates additional N and P inputs between the coast and the well locations. Additionally, the elevated ^{222}Rn activity in Black Point SGD suggests a different aquifer ^{222}Rn production rate compared to the upland wells which show much lower activities (22 – 150 dpm L^{-1}). This may be due to a change in geology and possibly geochemistry proximal to the coast. While the addition of nutrients is not dependent on the increased ^{222}Rn levels at Black Point, the presence of the two are possibly related. Wastewater sources

Table 7

Total SGD flux estimates for each site compared to total recharge rates for each aquifer watershed.

Site	Total SGD flux per site $\text{m}^3 \text{ d}^{-1}$	Total recharge $\text{m}^3 \text{ d}^{-1}$	SGD flux as a percentage of total recharge
Waialae West Aquifer _{upper}	–	16,000	–
Waialae West Aquifer _{lower}	–	4,400	–
Waialae West Aquifer _{total} —Black Point	15,000	20,000	75
Waialae East Aquifer—Kawaikui	5,000	9,000	55
Waialae East Aquifer—Wailupe	13,000	16,000	81

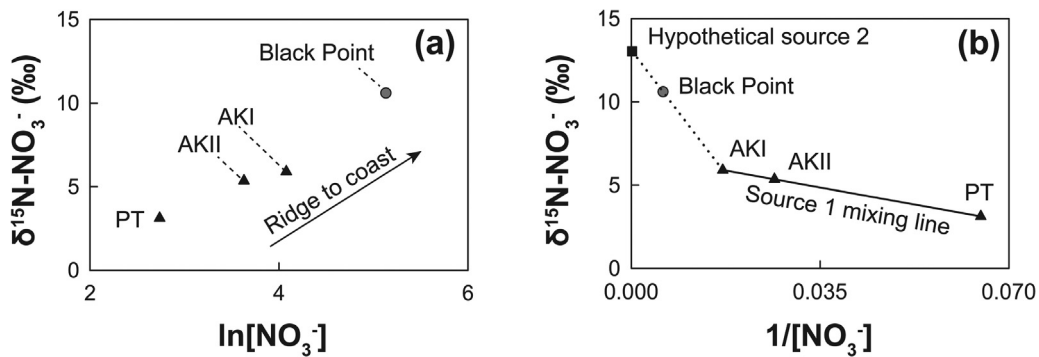


Fig. 6. (a) The natural logarithm of NO_3^- concentration versus $\delta^{15}\text{N-NO}_3^-$ values for Waialae West Aquifer groundwater. (b) Relationship between the inverse of NO_3^- concentration and $\delta^{15}\text{N-NO}_3^-$ values for Waialae West Aquifer groundwater. The solid line represents the mixing relationship between Palolo Tunnel and Aina Koa I. The dotted line represents the mixing relationship between the Black Point SGD endmember and Aina Koa I, and is extended out to approximate where the hypothetical second source's endmember falls (Eq. (3)).

may produce reducing groundwater conditions that mobilize iron and manganese. These elements capture radium as they are oxidized, producing a local ^{222}Rn source (Dulaiova et al., 2008; Gonnea et al., 2008). Oxygen concentrations at Black Point were slightly reduced relative to up-gradient groundwater (Table 3).

5.3. $\delta^{15}\text{N-NO}_3^-$ values as a proxy of NO_3^- source in the Waialae East Aquifer

All sites exhibited uniformity in $\delta^{15}\text{N-NO}_3^-$ values between SGD and recipient coastal waters, indicating that SGD is the dominant N source and that although SGD may emanate from several vents, it originates from a common source at each location. While no terrestrial groundwater data exist for the Waialae East Aquifer, well nutrient compositions may be analogous to that of Waialae West Aquifer as the areas are similarly affected by urbanization and hydrologically constrained by comparable climate patterns and lithology. Similarities between Wailupe SGD, Kawaikui SGD, and the well series geochemical compositions provide evidence of a common dominant N source or pathway. Kawaikui, Wailupe, and Aina Koa I and II have indistinguishable $\delta^{15}\text{N-NO}_3^-$ values and similar N concentrations which most closely resemble a soil N source. Typical isotopic values for soil $\delta^{15}\text{N-NO}_3^-$ range from 3 to 8% while fertilizers cover a slightly larger range from -4 to 4% (Freyer and Aly, 1974; Heaton, 1986; Kendall and McDonnell, 1998). Without upland well data in the Waialae East Aquifer, however, it is difficult to decipher if the measured NO_3^- stable isotope values at Kawaikui and Wailupe originate from similar source types as those in Waialae West Aquifer and if these NO_3^- stable isotope values are indicative of a soil N source rather than fertilizer or dilute wastewater-derived N.

5.4. $\delta^{15}\text{N-NO}_3^-$ values as a proxy of NO_3^- source in the Waialae West Aquifer

Although $\delta^{15}\text{N-NO}_3^-$ and $\delta^{18}\text{O-NO}_3^-$ values can be ambiguous as stand-alone indicators of NO_3^- source, especially if values overlap known ranges for more than one source type, the large spatial distinction in NO_3^- stable isotope ratios and elevated NO_3^- levels at Black Point clearly indicate an additional source or biogeochemical process separate from that of the other sites sampled. The values identified at Black Point overlap with past studies that report wastewater $\delta^{15}\text{N-NO}_3^-$ values of 10 to 20% (Aravena et al., 1993; Kendall and McDonnell, 1998; Kreitler et al., 1978; Kreitler and Browning, 1983). The elevated $\delta^{15}\text{N-NO}_3^-$ and $\delta^{18}\text{O-NO}_3^-$ values at Black Point do not appear to be the result of single-source fractionation processes such as denitrification. Differentiating between fractionation of a NO_3^- source and mixing of sources can be done graphically by comparing the natural logarithm of NO_3^- concentration and the inverse of NO_3^- concentration to $\delta^{15}\text{N-NO}_3^-$ values (Kendall and McDonnell, 1998). Denitrification of NO_3^- in Black Point SGD would manifest as elevated $\delta^{15}\text{N-NO}_3^-$ values and low NO_3^- concentrations relative to the upland wells sampled (Fig. 6a). Instead, the high $\delta^{15}\text{N-NO}_3^-$ values found at Black Point correspond to higher NO_3^- levels than those found up-gradient, indicating the addition of NO_3^- with elevated $\delta^{15}\text{N-NO}_3^-$ values closer to the coast. The coupled NO_3^- concentration and $\delta^{15}\text{N-NO}_3^-$ values observed in the Waialae West Aquifer support simple two-component mixing between the Palolo Tunnel endmember and a hypothetical high NO_3^- concentration, high $\delta^{15}\text{N-NO}_3^-$ value source (Fig. 6b). While there do not appear to be net fractionation processes occurring between the sites sampled, the source of the elevated NO_3^- stable isotope signature in Black Point SGD may still potentially originate from either a wastewater or denitrified fertilizer source. The observed NO_3^- stable isotope ratios at Black Point could be the result of mixing with a denitrified fertilizer source under the assumptions that there are sufficient chemical species to act as an electron donor as well as suboxic to anoxic conditions in the infiltration zone. We predicted the original fertilizer source NO_3^- concentration needed to account for the observed NO_3^- stable isotope ratios and NO_3^-

Table 8

Total number and types of on-site disposal systems in each aquifer.

Site	Aerobic	Cesspool	Multiple	Soil	Septic
Waialae West Aquifer _{upper}	–	25	–	–	–
Waialae West Aquifer _{lower}	2	260	5	13	23
Waialae West Aquifer _{total} —Black Point	2	285	5	13	23
Waialae East Aquifer—Kawaikui	–	9	–	–	1
Waialae East Aquifer—Wailupe	–	40	1	–	–

concentrations at Black Point. A hypothetical denitrified fertilizer source NO_3^- concentration of 739 μM was estimated using a simple mass balance as follows:

$$C_2 = \frac{(C_3 R_3 - C_1 R_1)}{R_2} \quad (2)$$

where C_1 is the NO_3^- concentration in Waialae West Aquifer_{upper} (Aina Koa I NO_3^- concentration, 59 μM), C_2 is the NO_3^- concentration in Waialae West Aquifer_{lower} (fertilizer NO_3^- input), C_3 is the cumulative NO_3^- concentration (zero-salinity Black Point SGD NO_3^- concentration, 195 μM), R_1 is the fraction of recharge in Waialae West Aquifer_{upper} (0.8), R_2 is the fraction of recharge in Waialae West Aquifer_{lower} (0.2), and R_3 is the total fraction of recharge (1). Recharge values are listed in Table 7 and separated based on the boundaries defined in Fig. 1c. This mass balance assumes that all recharge in Waialae West Aquifer_{lower} is affected equally by denitrified fertilizer leachate. A hypothetical denitrified fertilizer source $\delta^{15}\text{N}-\text{NO}_3^-$ value was then approximated using the mixing relationship between the Black Point SGD endmember and Aina Koa I $\delta^{15}\text{N}-\text{NO}_3^-$ and $1/[\text{NO}_3^-]$ values (Fig. 6b). The mixing line is defined as:

$$\delta^{15}\text{N}-\text{NO}_3^- = -425.1 \left(\frac{1}{[\text{NO}_3^-]} \right) + 13.1 \quad (3)$$

where the hypothetical source $\delta^{15}\text{N}-\text{NO}_3^-$ value is equal to 12.6‰. A simplified Rayleigh equation was used to calculate the original fertilizer NO_3^- concentration in recharge based on an enrichment factor within the range for denitrification of groundwater and a $\delta^{15}\text{N}-\text{NO}_3^-$ value commonly reported for fertilizer sources:

$$\delta = \delta_0 + \epsilon \ln \left(\frac{C}{C_0} \right) \quad (4)$$

where δ is the denitrified source $\delta^{15}\text{N}-\text{NO}_3^-$ value (12.6‰), δ_0 is the initial source $\delta^{15}\text{N}-\text{NO}_3^-$ value (0‰), ϵ is the enrichment factor (−25‰), C is the denitrified source NO_3^- concentration (739 μM) and C_0 is the initial fertilizer NO_3^- concentration (Aravena and Robertson, 1998; Böttcher et al., 1990; Kendall and McDonnell, 1998; Mengis et al., 1999; Vogel et al., 1981). An original fertilizer NO_3^- concentration of 1,223 μM would be needed to account for the assumed denitrified fertilizer NO_3^- concentration and $\delta^{15}\text{N}-\text{NO}_3^-$ value. Specific to O'ahu, a groundwater N concentration of 1,223 μM far exceeds the maximum groundwater N concentration of 543 μM observed beneath intensely cultivated fields in the Pearl Harbor Aquifer (Ling, 1996). Fertilizer NO_3^- concentrations of this magnitude are typically only found in groundwater severely impacted by intensive agricultural practices (Liao et al., 2012; Valiela and Bowen, 2002). Black Point has no history of intensive agriculture, however, and the suboxic to anoxic conditions necessary for denitrification were not observed in any groundwater sampled in the Waialae West Aquifer (Table 3) (Frans et al., 2012). This denitrified fertilizer source hypothesis is highly improbable based on the above discussion as well as known land-use characteristics that instead depict a high prevalence of OSDS sites in the Waialae West Aquifer.

5.5. Wastewater as a NO_3^- source in the Waialae West Aquifer

The majority of OSDS in the Black Point area are in the form of cesspools with nearly 118 units residing on parcels within 1 km of the sampling location and 82 units within 500 m. The potential effects of wastewater leachate on Black Point SGD composition are particularly evident when comparing the total OSDS sites in the watersheds of both Wailupe and Kawaikui which cumulatively amount to 51 units, or just 16% of the approximately 328 OSDS units in the Waialae West Aquifer (Table 8). Three hypothetical sewage NO_3^- concentrations were considered based on minimum, average, and maximum DIN values reported for cesspools in previous studies to quantify corresponding hypothetical source $\delta^{15}\text{N}-\text{NO}_3^-$ values using Eq. (3): 1,100 μM , 4,300 μM , and 7,300 μM (Lowe et al., 2009; Whittier and El-Kadi, 2009; WRCC, 2008). Since NO_3^- was the predominant constituent of DIN in Black Point SGD (NH_4^+ composed less than 0.1% of DIN), we assume that any original NH_4^+ from the cesspools underwent nitrification. As such, cesspool DIN concentrations were assumed to equal NO_3^- concentrations. Aina Koa I NO_3^- concentrations and $\delta^{15}\text{N}-\text{NO}_3^-$ values were chosen to represent the aggregate source end-member signature of upland groundwater aside from wastewater effluent as 80% of recharge occurs up-gradient of Aina Koa I. Predicted $\delta^{15}\text{N}-\text{NO}_3^-$ values for the cesspool source ranged from 12.7–13.1‰ depending on cesspool NO_3^- concentration. These $\delta^{15}\text{N}-\text{NO}_3^-$ values are consistent with previously published values for the wastewater sources discussed above.

Table 9

Model-derived values for recharge and wastewater in each aquifer or watershed. Wastewater contributions are expressed as percentage of total recharge.

Site	Recharge m ³ d ⁻¹	Wastewater recharge m ³ d ⁻¹	Wastewater recharge as a percentage of total recharge
Waialae West Aquifer _{upper}	16,000	68	0.4
Waialae West Aquifer _{lower}	3,600	850	19
Waialae West Aquifer _{total} —Black Point	20,000	920	4.4
Waialae East Aquifer—Kawaikui	9,000	30	0.3
Waialae East Aquifer—Wailupe	16,000	110	0.7

Table 10

Total N fluxes for wastewater effluent and recharge in each aquifer or watershed compared to total SGD TDN loadings at each coastal site.

Site	Wastewater N load kg d ⁻¹	Recharge N load kg d ⁻¹	Total N load kg d ⁻¹	SGD TDN load kg d ⁻¹	SGD TDN as a percentage of total N
Waialae West Aquifer _{upper}	4.2	20	24	—	—
Waialae West Aquifer _{lower}	46	23	69	—	—
Waialae West Aquifer _{total} —Black Point	50	43	93	38	41
Waialae East Aquifer—Kawaikui	1.7	—	—	4.0	—
Waialae East Aquifer—Wailupe	6.3	—	—	14	—

Table 11

Total P fluxes for wastewater effluent and recharge in each aquifer or watershed compared to total SGD TDP loadings at each coastal site.

Site	Wastewater P load kg d ⁻¹	Recharge P load kg d ⁻¹	Total P load kg d ⁻¹	SGD TDP load kg d ⁻¹	SGD TDP as a percentage of total P
Waialae West Aquifer _{upper}	1.2	0.6	1.8	—	—
Waialae West Aquifer _{lower}	13	0.2	13	—	—
Waialae West Aquifer _{total} —Black Point	14	0.8	15	1.7	11
Waialae East Aquifer—Kawaikui	0.5	—	—	0.9	—
Waialae East Aquifer—Wailupe	1.7	—	—	0.8	—

The recharge model was used to determine the relative volumetric contributions of wastewater effluent in each groundwater basin (Engott et al., 2015; Whittier and El-Kadi, 2009). Wastewater effluent accounted for 4.4% of total recharge in the entire Waialae West Aquifer compared to just 0.7% and 0.3% of Waialae East Aquifer—Wailupe and Waialae East Aquifer—Kawaikui, respectively (Table 9). As such, denitrification of a wastewater source in Waialae West Aquifer is unlikely, even if the source itself is anoxic, as sewage effluent is diluted at a ratio of 1:23 by up-gradient oxic groundwater. To substantiate the aquifer-scale estimates, we calculated the relative volumetric contribution of the wastewater source solely based on NO₃[−] concentrations in the aquifer using the following equation:

$$F_w = \frac{(C_2 - C_1)}{(C_3 - C_1)} \quad (5)$$

where F_w is the fraction of NO₃[−] originating from wastewater, C_1 is the first source's NO₃[−] concentration (Aina Koa I NO₃[−] concentration, 59 μM), C_2 is the intermediate NO₃[−] concentration (zero-salinity Black Point SGD NO₃[−] concentration, 195 μM), and C_3 is the second source's NO₃[−] concentration (sewage NO₃[−] concentrations, 1,100–7,300 μM). This method suggests that 2–13% of groundwater is contributed by sewage effluent. This range encompasses the 4.4% calculated based on recharge fractions. In comparison, we calculated the exact NO₃[−] content needed to account for the 4.4% wastewater effluent observed in the Waialae West Aquifer to be 3,150 μM by rearranging Eq. (5). A cesspool source that contributes 3,150 μM of NO₃[−] to the underlying aquifer as opposed to the higher concentrations cited above is possible as N from OSDS leachate may be attenuated in the vadose zone through minimally fractionating processes close to the source (e.g. sorption of ammonium, immobilization of organic N). Additionally, these estimates assume that N is well-homogenized within the aquifer between each source. While this may be true for the upper region of Black Point, the distribution and concentration of OSDS units along the coast likely exhibit a disproportional, proximal effect on Black Point SGD that may not be well represented by the recharge and effluent volumetric ratios. While the exact proportion of wastewater in SGD at Black Point cannot be precisely defined based on existing data, there is strong evidence that supports that Black Point SGD is influenced by OSDS leachate.

Modeled TN and TP fluxes from wastewater effluent were compiled for each aquifer to evaluate the significance of total SGD N and P loads as a percentage of total N and P loads in each aquifer. Background N and P loads were accounted for by spatially parsing out fluxes in the following areas of the Waialae West Aquifer: (1) Ko'olau Ridge-Palolo Tunnel, (2) Palolo Tunnel-Aina Koa II, and (3) Aina Koa II-coast (Fig. 1c). We iteratively solved for recharge TDN and TDP concentrations based on observed well concentrations in the areas defined above using a simple mass balance. Background N and P fluxes were calculated by multiplying the recharge volume for each spatial component by recharge concentration and then adding wastewater derived N and P fluxes to determine total fluxes. SGD N and P contributions were quantified by multiplying total SGD fluxes by the SGD endmember concentrations at each site from Table 3. At Black Point, SGD delivered nearly 40% of total N and 11% of total P in the Waialae West Aquifer, a reflection of the conservative nature of N and non-conservative behavior

of P in the subsurface as well as the large overall fraction of recharge that discharges at Black Point ([Tables 10 and 11](#)). Both Kawaikui's and Wailupe's SGD N fluxes were larger than prescribed by wastewater effluent alone. We suspect the presence of an additional source that is well-homogenized between the areas, such as soil N, supplying relatively low nutrient concentrations to the coast similar in form to Aina Koa I's nutrient composition.

$\delta^{18}\text{O}-\text{NO}_3^-$ values were unclear in interpretation of NO_3^- source in groundwater in this study. Complex biogeochemical cycling often interferes and attenuates the original O signature and measured $\delta^{18}\text{O}-\text{NO}_3^-$ values are typically highly-altered from original compositions in the subsurface ([Minet et al., 2012](#)). In the case of sewage-derived NO_3^- , the amine group containing ^{15}N in urea is mineralized to ammonia and subsequently nitrified to NO_3^- . As this occurs, O from both atmospheric oxygen and water may be incorporated into the resultant NO_3^- , altering its O isotopic content ([Kool et al., 2007, 2011](#)). As such, the elevated $\delta^{18}\text{O}-\text{NO}_3^-$ values observed at Black Point relative to the other coastal sites could represent a difference in fractionation processes such as the inclusion of atmospheric oxygen or exchange with oxygen in water.

5.6. Behavior of SGD-delivered nutrients in nearshore waters

Nutrient distributions varied with salinity at each site and showed evidence of non-conservative behavior for NO_3^- , NH_4^+ , and SiO_4^{4-} . At Black Point and Wailupe, negative residuals in NO_3^- and SiO_4^{4-} content overlapped with positive residuals in NH_4^+ in mid-salinity waters. The negative residual NO_3^- content may be an indication of autotrophic utilization. While SGD conveyed negligible amounts of NH_4^+ , there were large deviations in NH_4^+ concentrations from mixing lines in brackish waters at all sites. Salinity-mediated desorption of NH_4^+ from sediments may be responsible for the observed peaks of NH_4^+ at mid-salinity ranges between the three sites. NH_4^+ adsorbs onto sediments at low salinities when the activity of competing ions is low and becomes entrained in more saline waters as competition for particle exchange sites from other ions increases ([Boatman and Murray, 1982](#); [Seitzinger et al., 1991](#); [Weston et al., 2010](#)). Alternatively, the non-conservative behavior of NH_4^+ may provide evidence of local production in coastal waters. Although residuals in PO_4^{3-} content indicated non-conservative behavior at each location, there were no clear trends in the magnitude and direction of the residuals. Similarly, NH_4^+ and SiO_4^{4-} residuals did not reveal clear relationships at Kawaikui. At Black Point and Kawaikui, SiO_4^{4-} concentrations showed large deviations from mixing lines in mid-salinity waters and may provide supporting evidence of biological assimilation of SGD-conveyed nutrients such as NO_3^- in coastal waters.

6. Conclusion

These findings illustrate the utility of synthesizing SGD nutrient fluxes and NO_3^- stable isotope parameters together with land-use and recharge data in determining the contribution of terrestrial sources to coastal nutrient loading via SGD. In addition to exploring nutrient dynamics for each study site, we demonstrate that OSDS leachate is likely responsible for the elevated SGD N content observed at Black Point. These results should aid in restoration efforts aimed at curbing nutrient pollution in Maunalua Bay by providing regulators with source determination information. Additionally, these findings shed light on the magnitude and spatial variability of SGD-conveyed nutrients to coastal waters in the study area and allow us to better understand the capacity of these nutrients to perturb nearshore ecological dynamics. Future efforts should address potential biogeochemical transformations in similar nearshore environments affected by elevated SGD N and P loads.

Acknowledgments

The authors thank Joseph Fackrell and Brian Popp who provided valuable technical assistance to this project. We thank Samuel Wall, Florybeth La Valle, Trista McKenzie, Chad Moore, Katie Lubarsky, and Nyssa Silbiger for field assistance. We recognize Nancy Matsumoto and Kenneth Tom at the Honolulu Board of Water Supply for graciously providing access to wells for sampling. This paper was funded in part by a grant from the NOAA, Project #R/SB-11, which is sponsored by the University of Hawai'i Sea Grant College Program, SOEST, under Institutional Grant No. NA140AR4170071 (UNIHI-SEAGRANT-JC-15-01) from the NOAA Office of Sea Grant, Department of Commerce with additional support provided by the National Science Foundation Graduate Research Fellowship Program (DGE-1329626), and the Harold T. Stearns Fellowship. The views expressed herein are those of the authors and do not necessarily reflect the views of NOAA or any of its sub-agencies.

References

- Aravena, R., Evans, M., Cherry, J.A., 1993. Stable isotopes of oxygen and nitrogen in source identification of nitrate from septic systems. *Groundwater* 31 (2), 180–186.
- Aravena, R., Robertson, W.D., 1998. Use of multiple isotope tracers to evaluate denitrification in ground water: study of nitrate from a large-flux septic system plume. *Groundwater* 36 (6), 975–982.
- Armstrong, F., Stearns, C., Strickland, J., 1967. The measurement of upwelling and subsequent biological process by means of the technicon autoanalyzer® and associated equipment. In: Deep Sea Research and Oceanographic Abstract. Elsevier, pp. 381–389.
- Ateweberhan, M., et al., 2013. Climate change impacts on coral reefs: synergies with local effects, possibilities for acclimation, and management implications. *Mar. Pollut. Bull.* 74 (2), 526–539.
- Atkinson, A., 2007. A Natural and Cultural History of Maunalua Bay and its Watershed. Ph.D. Dissertation. San Francisco State University, Department of Geography.

- Beusen, A.H.W., Slomp, C.P., Bouwman, A.F., 2013. Global land–ocean linkage: direct inputs of nitrogen to coastal waters via submarine groundwater discharge. *Environ. Res. Lett.* 8 (3), 034035.
- Boatman, C.D., Murray, J.W., 1982. Modeling exchangeable NH⁴⁺ adsorption in marine sediments: process and controls of adsorption1, 2. *Limnol. Oceanogr.* 27 (1), 99–110.
- Böhlke, J., Mroczkowski, S., Coplen, T., 2003. Oxygen isotopes in nitrate: new reference materials for 18O:17O:16O measurements and observations on nitrate–water equilibration. *Rapid Commun. Mass Spectrom.* 17 (16), 1835–1846.
- Böttcher, J., Strebel, O., Voerkelius, S., Schmidt, H.L., 1990. Using isotope fractionation of nitrate-nitrogen and nitrate-oxygen for evaluation of microbial denitrification in a sandy aquifer. *J. Hydrol.* 114 (3), 413–424.
- Burnett, W., Kim, G., Lane-Smith, D., 2001. A continuous monitor for assessment of 222Rn in the coastal ocean. *J. Radioanal. Nucl. Chem.* 249 (1), 167–172.
- Burnett, W.C., Dulaiova, H., 2003. Estimating the dynamics of groundwater input into the coastal zone via continuous radon-222 measurements. *J. Environ. Radioact.* 69 (1), 21–35.
- Casciotti, K., Sigman, D., Hastings, M.G., Böhlke, J., Hilkert, A., 2002. Measurement of the oxygen isotopic composition of nitrate in seawater and freshwater using the denitrifier method. *Anal. Chem.* 74 (19), 4905–4912.
- Cesar, H.S., Van Beukering, P., 2004. Economic valuation of the coral reefs of Hawai'i. *Pac. Sci.* 58 (2), 231–242.
- Cole, M.L., Kroeger, K.D., McClelland, J.W., Valiela, I., 2006. Effects of watershed land use on nitrogen concentrations and δ¹⁵ nitrogen in groundwater. *Biogeochemistry* 77 (2), 199–215.
- Corbett, D.R., et al., 1999. Patterns of groundwater discharge into Florida Bay. *Limnol. Oceanogr.* 44 (4), 1045–1055.
- Dimova, N.T., Swarzenski, P.W., Dulaiova, H., Glenn, C.R., 2012. Utilizing multichannel electrical resistivity methods to examine the dynamics of the fresh water-seawater interface in two Hawaiian groundwater systems. *J. Geophys. Res. Oceans* 117 (C2), 1978–2012.
- Dulaiova, H., Gonnea, M.E., Henderson, P.B., Charette, M.A., 2008. Geochemical and physical sources of radon variation in a subterranean estuary—implications for groundwater radon activities in submarine groundwater discharge studies. *Mar. Chem.* 110 (1), 120–127.
- Engott, J.A., Johnson, A.G., Bassiouni, M., Izuka, S.K., 2015. Spatially distributed groundwater recharge for 2010 land cover estimated using a water-budget model for the island of O'ahu, Hawai'i. *US Geol. Survey*, 2328.
- Eyre, P.R., Ewart, C.J., Shadé, P.J., 1986. Hydrology of the Leeward Aquifers of Southeast Oahu, Hawai'i. *US Geol. Surv.*, 85–4270.
- Frans, L.M., Rupert, M.G., Hunt Jr, C.D., Skinner, K.D., 2012. Groundwater quality in the Columbia Plateau, Snake River Plain, and Oahu basaltic-rock and basin-fill aquifers in the Northwestern United States and Hawai'i, 1992–2010. US Geological Survey Scientific Investigations Report, 201.
- Freyer, H.D., Aly, A., 1974. Nitrogen-15 variations in fertilizer nitrogen. *J. Environ. Qual.* 3 (4), 405–406.
- Ganguli, P.M., Swarzenski, P.W., Dulaiova, H., Glenn, C.R., Flegal, A.R., 2014. Mercury dynamics in a coastal aquifer: Maunalua Bay, O'ahu, Hawai'i. *Estuarine, Coast. Shelf Sci.* 140, 52–65.
- Giambelluca, T.W., et al., 2013. Online rainfall atlas of Hawai'i. *Bull. Am. Meteorol. Soc.* 94 (3), 313–316.
- Giambelluca, T.W., et al., 2014. Evapotranspiration of Hawai'i. Final report submitted to U.S. Army Corps of Engineers—Honolulu District and the Commission on Water Resource Management, State of Hawai'i.
- Gonnea, M.E., Morris, P.J., Dulaiova, H., Charette, M.A., 2008. New perspectives on radium behavior within a subterranean estuary. *Mar. Chem.* 109 (3), 250–267.
- Grasshoff, K., Kremling, K., Ehrhardt, M., 2009. *Methods of Seawater Analysis*, Second ed. Verlag Chemie GmbH, Weinheim, 419 pp.
- Hawai'i Department of Health (HDOH), 2004. Hawai'i Administrative Rules, Title 11, Department of Health, Chapter 62, Wastewater Systems.
- Heaton, T.H., 1986. Isotopic studies of nitrogen pollution in the hydrosphere and atmosphere: a review. *Chem. Geol. Isotope Geosci. Sect.* 59, 87–102.
- Holleman, K., 2011. Impact of flux, residence time and nutrient load of submarine groundwater discharge on coastal phytoplankton growth in coastal waters of Hawai'i. Master's Thesis, University of Hawai'i at Mānoa, Honolulu, Hawai'i.
- Hughes, T.P., et al., 2003. Climate change, human impacts, and the resilience of coral reefs. *Science* 301 (5635), 929–933.
- Hwang, D.W., Kim, G., Lee, Y.W., Yang, H.S., 2005. Estimating submarine inputs of groundwater and nutrients to a coastal bay using radium isotopes. *Mar. Chem.* 96 (1), 61–71.
- Johannes, R., 1980. Ecological significance of the submarine discharge of groundwater. *Mar. Ecol. Prog. Ser.* 3 (4), 365–373.
- Kendall, C., McDonnell, J.J., 1998. *Isotope Tracers in Catchment Hydrology*. Elsevier Science B.V., Amsterdam, pp. 839.
- Kéroutil, R., Aminot, A., 1997. Fluorometric determination of ammonia in sea and estuarine waters by direct segmented flow analysis. *Mar. Chem.* 57 (3), 265–275.
- Kim, G., Lee, K.K., Park, K.S., Hwang, D.W., Yang, H.S., 2003. Large submarine groundwater discharge (SGD) from a volcanic island. *Geophys. Res. Lett.* 30 (21).
- Knee, K.L., Street, J.H., Boehm, A.B., Paytan, A., 2010. Nutrient inputs to the coastal ocean from submarine groundwater discharge in a groundwater-dominated system: relation to land use (Kona Coast, Hawaii, USA). *Limnol. Oceanogr.* 55 (3), 1105–1122.
- Kool, D.M., Wragge, N., Oenema, O., Dolfig, J., Van Groenigen, J.W., 2007. Oxygen exchange between (de) nitrification intermediates and H₂O and its implications for source determination of NO₃⁻ and N₂O: a review. *Rapid Commun. Mass Spectrom.* 21 (22), 3569–3578.
- Kool, D.M., Wragge, N., Oenema, O., Van Kessel, C., Van Groenigen, J.W., 2011. Oxygen exchange with water alters the oxygen isotopic signature of nitrate in soil ecosystems. *Soil Biol. Biochem.* 43 (6), 1180–1185.
- Kreitler, C.W., Ragone, S.E., Katz, B.G., 1978. N15/N14 ratios of ground-water nitrate, Long Island, New York. *Groundwater* 16 (6), 404–409.
- Kreitler, C.W., Browning, L.A., 1983. Nitrogen-isotope analysis of groundwater nitrate in carbonate aquifers: natural sources versus human pollution. *J. Hydrol.* 61 (1), 285–301.
- Krest, J.M., Moore, W., Gardner, L., Morris, J., 2000. Marsh nutrient export supplied by groundwater discharge: evidence from radium measurements. *Global Biogeochem. Cycl.* 14 (1), 167–176.
- Lapointe, B.E., Clark, M.W., 1992. Nutrient inputs from the watershed and coastal eutrophication in the Florida keys. *Estuaries* 15 (4), 465–476.
- Lee, J.M., Kim, G., 2007. Estimating submarine discharge of fresh groundwater from a volcanic island using a freshwater budget of the coastal water column. *Geophys. Res. Lett.* 34 (11).
- Liao, L., Green, C.T., Belkins, B.A., Böhlke, J., 2012. Factors controlling nitrate fluxes in groundwater in agricultural areas. *Water Resour. Res.* 48 (6).
- Ling, G., 1996. Assessment of nitrate leaching in the unsaturated zone on Oahu—Water. Resources Research Center Technical Report—WRRC-96-08. University of Hawai'i at Mānoa, Honolulu, Hawai'i.
- Lowe, K.S., Tucholke, M.B., Tomaras, J.M., 2009. Influent Constituent Characteristics of the Modern Waste Stream from Single Sources. Water Environment Research Foundation.
- McClelland, J.W., Valiela, I., Michener, R.H., 1997. Nitrogen-stable isotope signatures in estuarine food webs: a record of increasing urbanization in coastal watersheds. *Limnol. Oceanogr.* 42 (5), 930–937.
- McCook, L., 1999. Macroalgae, nutrients and phase shifts on coral reefs: scientific issues and management consequences for the Great Barrier Reef. *Coral Reefs* 18 (4), 357–367.
- McIlvin, M.R., Casciotti, K.L., 2010. Fully automated system for stable isotopic analyses of dissolved nitrous oxide at natural abundance levels. *Limnol. Oceanogr. Methods* 8 (2), 54–66.
- McIlvin, M.R., Casciotti, K.L., 2011. Technical updates to the bacterial method for nitrate isotopic analyses. *Anal. Chem.* 83 (5), 1850–1856.
- Mengis, M., et al., 1999. Multiple geochemical and isotopic approaches for assessing ground water NO₃-elimination in a riparian zone. *Groundwater* 37 (3), 448–457.
- Metcalf, Eddy, 1991. *Wastewater Engineering – Treatment, Disposal, and Reuse*, 3rd edition. McGraw-Hill, New York, NY, pp. 15–46, Inc.
- Minet, E., et al., 2012. Evaluating the utility of 15 N and 18 O isotope abundance analyses to identify nitrate sources: a soil zone study. *Water Res.* 46 (12), 3723–3736.

- Moore, W.S., 1999. The subterranean estuary: a reaction zone of ground water and sea water. *Mar. Chem.* 65 (1), 111–125.
- Murphy, J., Riley, J., 1962. A modified single solution method for the determination of phosphate in natural waters. *Anal. Chim. Acta* 27, 31–36.
- Nelson, C.E., et al., 2015. Fluorescent dissolved organic matter as a multivariate biogeochemical tracer of submarine groundwater discharge in coral reef ecosystems. *Mar. Chem.*
- Nicholls, R.J., et al., 2007. Coastal systems and low lying areas. *Climate Change 2007. Impacts Adaptation Vulnerability*, 315–357.
- Nichols, W.D., Shade, P.J., Hunt, C.D., 1997. Summary of the Oahu Hawai'i, regional aquifer-system analysis, 1412. USGPO.
- Pandolfi, J.M., et al., 2003. Global trajectories of the long-term decline of coral reef ecosystems. *Science* 301 (5635), 955–958.
- Paytan, A., et al., 2006. Submarine groundwater discharge: an important source of new inorganic nitrogen to coral reef ecosystems. *Limnol. Oceanogr.* 51 (1), 343–348.
- Rodellas, V., Garcia-Orellana, J., Masqué, P., Feldman, M., Weinstein, Y., 2015. Submarine groundwater discharge as a major source of nutrients to the Mediterranean Sea. *Proc. Natl. Acad. Sci.* 112 (13), 3926–3930.
- Schubert, M., Paschke, A., Lieberman, E., Burnett, W.C., 2012. Air–water partitioning of ^{222}Rn and its dependence on water temperature and salinity. *Environ. Sci. Technol.* 46 (7), 3905–3911.
- Seitzinger, S.P., Gardner, W.S., Spratt, A.K., 1991. The effect of salinity on ammonium sorption in aquatic sediments: implications for benthic nutrient recycling. *Estuaries* 14 (2), 167–174.
- Sigman, D., et al., 2001. A bacterial method for the nitrogen isotopic analysis of nitrate in seawater and freshwater. *Anal. Chem.* 73 (17), 4145–4153.
- Slomp, C.P., Van Cappellen, P., 2004. Nutrient inputs to the coastal ocean through submarine groundwater discharge: controls and potential impact. *J. Hydrol.* 295 (1), 64–86.
- Smith, J., Smith, C., Hunter, C., 2001. An experimental analysis of the effects of herbivory and nutrient enrichment on benthic community dynamics on a Hawaiian reef. *Coral Reefs* 19 (4), 332–342.
- Stearns, H., Vaksvik, K.N., 1935. Geology and ground-water resources of the Island of Oahu, Hawai'i. Div. Hydrogr. Bull. 1, 479.
- Swarzenski, P.W., et al., 2013. A geochemical and geophysical assessment of coastal groundwater discharge at select sites in Maui and Oahu, Hawai'i. *Groundw. Coast. Zones Asia-Pac.*, 27–46.
- Takasaki, K.J., Mink, J.F., 1982. Water resources of southeastern Oahu, Hawai'i. 2331–1258. US Geol. Surv.
- Taniguchi, M., et al., 2008. Groundwater discharge as an important land-sea pathway into Manila Bay, Philippines. *J. Coast. Res.* 24, 15–24.
- Valiela, I., Bowen, J.L., 2002. Nitrogen sources to watersheds and estuaries: role of land cover mosaics and losses within watersheds. *Environ. Pollut.* 118 (2), 239–248.
- Vogel, J., Talma, A., Heaton, T., 1981. Gaseous nitrogen as evidence for denitrification in groundwater. *J. Hydrol.* 50, 191–200.
- Weston, N.B., Giblin, A.E., Banta, G.T., Hopkinson, C.S., Tucker, J., 2010. The effects of varying salinity on ammonium exchange in estuarine sediments of the Parker River, Massachusetts. *Estuaries Coasts* 33 (4), 985–1003.
- Whittier, R.B., El-Kadi, A.I., 2009. Human and Environmental Risk Ranking of Onsite Sewage Disposal Systems. Final report submitted to State of Hawai'i Department of Health, Safe Drinking Water Branch, Honolulu, Hawai'i.
- Wolanski, E., Martinez, J.A., Richmond, R.H., 2009. Quantifying the impact of watershed urbanization on a coral reef: Maunalua Bay, Hawai'i. *Estuarine Coast. Shelf Sci.* 84 (2), 259–268.
- WRRC and Engineering Solutions, Inc., 2008. Onsite Wastewater Treatment Survey and Assessment. Final report submitted to the State of Hawai'i, Department of Business, Economic Development and Tourism Office of Planning, Hawai'i Coastal Zone Management Program, and the Department of Health.
- Yu, Z., Raabe, T., Hemken, G., Brockmann, U., 2004. Continuous flow analysis of dissolved total phosphorus in seawater by UV-K2S2O8 online digestion method. *Acta Oceanol. Sin.* 23 (4), 637–645.